

# Momentum distribution of $N^*$ in nuclei

N. G. Kelkar

Departamento de Fisica, Universidad de los Andes, Cra 1E, 18A-10, Bogotá, Colombia

## Abstract

Due to its dominance in the low energy eta-nucleon interaction, the S11  $N^*(1535)$  resonance enters as an important ingredient in the analyses of experiments aimed at finding evidence for the existence of eta-mesic nuclei. The static properties of the resonance get modified inside the nucleus and its momentum distribution is used in deciding these properties as well as the kinematics in the analyses. Here we show that given the possibility for the existence of an  $N^*$ - $^3\text{He}$  quasibound state, the relative momentum distribution of an  $N^*$  and  $^3\text{He}$  inside such a  $^4\text{He}$  is narrower than that of neutron- $^3\text{He}$  in  $^4\text{He}$ . Results for the  $N^*$ - $^{24}\text{Mg}$  system are also presented. The present exploratory work could be useful in motivating searches of exotic  $N^*$ -nucleus quasibound states as well as in performing analyses of eta meson production data.

PACS numbers: 21.85.+d, 25.40.Ny

## I. INTRODUCTION

A few decades ago, a new topic in meson physics drew the attention of intermediate energy nuclear physicists. This was due to the finding that the interaction between the eta meson ( $\eta$ ) and a nucleon is strongly attractive [1] and that this interaction may generate sufficient attraction to give rise to an exotic bound state (also referred to as “quasibound” since it decays within a short time) when put in the nuclear environment. The prediction for the existence of such eta-mesic nuclei initiated lots of efforts on the experimental as well as the theoretical front [2, 3]. Due to the lack of eta beams (as the eta meson is extremely short lived), experiments where the  $\eta$  was produced in the final state with protons and photons incident on nuclei, were performed. However, apart from two controversial experiments [4], there has been no definite evidence for the existence of these states. Meanwhile, the interest has also shifted from  $\eta$  to  $\eta'$  mesic nuclei [5]. However, the WASA group [6] is still active in the search for eta-mesic states in light nuclei (see also [7] for theoretical works on eta-mesic helium nuclei).

Many a time in physics, an experimental finding is not a direct measurement but rather a result deduced from the analysis of experimental data using theoretical inputs. For example, nuclear radii are not “measured” but rather extracted [8] using theoretical relations involving electromagnetic form factors of nuclei which are deduced from data on electron-nucleus scattering. The experimental searches for eta-mesic nuclei involve certain assumptions and theoretical inputs too. One of the (sufficiently justified) assumption is that the interaction of the  $\eta$  meson with the nucleus proceeds through the formation of the S11  $N^*(1535)$  resonance. Hence, analyses of an anticipated eta mesic nucleus, model the eta-nucleon interaction to proceed via the formation of an  $N^*(1535)$  resonance which repeatedly decays, regenerates and propagates within the nucleus until it eventually decays into a free meson and a nucleon. The search for an  ${}^4\text{He}\text{-}\eta$  bound state which for example involves the analysis of the  $dd \rightarrow {}^3\text{He } N\pi$  reaction data, is performed by assuming that the reaction proceeds as follows [9]:  $dd \rightarrow ({}^4\text{He}\text{-}\eta)_{\text{bound}} \rightarrow ({}^3\text{He}\text{-}N^*) \rightarrow {}^3\text{He } N\pi$ . Thus it becomes necessary to incorporate the static properties and motion of the  $N^*$  resonance inside the nucleus. One essential ingredient in these analyses is the relative momentum distribution of  $N^*\text{-}{}^3\text{He}$  inside the  ${}^4\text{He}$  nucleus (which contains an  $N^*$  in place of one proton or neutron). This distribution is necessary to establish the detector system acceptance for the registration of the  $dd \rightarrow ({}^3\text{He}\text{-}N^*) \rightarrow {}^3\text{He}$

$N\pi$  reaction and to determine the data selection criteria [6]. However, with the knowledge of the  $N^*$  interaction with nucleons not being sufficient (see however the discussion in the next section), it is common to use the momentum distribution of a nucleon inside the nucleus rather than that of the resonance. In fact, even though the momentum distributions inside nuclei provide information which is complementary to that obtained from electromagnetic form factors, much less experimental information is available on the former even in normal nuclei.

In the present work, a model for the evaluation of the momentum distribution of an  $N^*$  inside a nucleus is presented. In a recent work [10], the possibility for the existence of broad  $N^*$ -nucleus (quasi)bound states was proposed using some available sets of coupling constants for the  $N N^* \rightarrow N N^*$  interaction. Since a few bound states in the  $N^*$ - $^3\text{He}$  and  $N^*$ - $^{24}\text{Mg}$  were indeed predicted, in this work we use these binding energies (as well as some others obtained by varying the coupling constants) to evaluate the momentum distribution of the  $N^*$  resonance in these nuclei. In the next section, we shall briefly repeat the formalism used in [10] and proceed further to describe the evaluation of the momentum distributions. An interesting outcome of these investigations is that the momentum distribution of an  $N^*$  resonance inside a nucleus is narrower than that of a nucleon inside a nucleus. This fact could indeed be of significant importance in the analyses done in connection with the searches for eta-mesic nuclei.

## II. MODEL FOR THE $N^*$ -NUCLEUS POTENTIAL

Though the existence of a bound state of a baryon resonance and a nucleus is by itself an exotic idea, it has indeed been explored in context with the  $\Delta$  (spin-isospin  $3/2$ ) resonance [11] in the past. In [12], the author calculated the momentum distribution of such a resonance too. As compared to the  $\Delta$ , the case of the  $N^*(1535)$  resonance is relatively simpler. It is a spin  $1/2$  (negative parity)  $S_{11}$  resonance which decays dominantly into a nucleon and a pion or eta meson. Hence, we shall use a one meson exchange  $N N^* \rightarrow N N^*$  interaction with the exchange of a  $\pi$  and  $\eta$  meson. The  $N^*$ -nucleus potential is then obtained by folding the elementary  $N N^*$  interaction with a nuclear density (see some remarks regarding the validity of the folding model in this work, above Eq.(9)). We shall also retain the scalar part of the interaction only. Since the  $N^*(1535)$  is a negative parity baryon, indeed in the one-pion

and  $\eta$ -exchange diagrams, the spin dependent terms are suppressed as compared to the leading scalar terms.

As for the  $\pi NN^*$  and  $\eta NN^*$  coupling constants, there appears a range of values in literature [13–19]. In the first reference in [14], for example, the cross sections for photoproduction of  $\eta$  mesons from heavy nuclei were measured and compared with models of the quasifree  $A(\gamma, p)X$  reaction. The authors adjusted the coupling constants from an Effective Lagrangian Approach (ELA) in [19] to reproduce the  $p(\gamma, \eta)p$  and  $d(\gamma, \eta)np$  data. With  $g_{\pi NN^*} = 0.699$  and  $g_{\eta NN^*} = 2.005$ , the experimental  $\eta$  photoproduction cross sections on complex nuclei were reproduced within the model of [19]. In the two references in [15], the authors found  $g_{\pi NN^*} = 0.8$  and  $g_{\eta NN^*} = 2.22$  while comparing the calculations within a one boson exchange model with the  $NN \rightarrow NN\eta$  and  $\pi^- p \rightarrow \eta n$  data. Somewhat bigger values of the  $\pi NN^*$  coupling constant have been found in more recent years with Ref. [16] for example, reporting  $g_{\pi NN^*} = 1.09$  by comparing calculations within a chiral constituent quark model with the experimental data on the partial decay width of the  $S_{11}(1535)$  resonance. Mixing pseudoscalar meson-baryon with vector meson-baryon states in a coupled channels scheme with  $\pi N$ ,  $\eta N$ ,  $K\Lambda$ ,  $K\Sigma$ ,  $\rho N$  and  $\pi\Delta$ , the coupling constants,  $g_{\pi NN^*} = 1.05$  and  $g_{\eta NN^*} = 1.6$  were obtained in [18]. In a study of nonstrange meson baryon systems where the  $N^*(1535)$  was found to get generated as a result of coupled channel dynamics of vector meson-baryon and pseudoscalar-baryon systems, the authors [17] obtain,  $g_{\pi NN^*} = 0.95$  and  $g_{\eta NN^*} = 1.77$ . We shall present results with some sets of coupling constants mentioned above. The constants and binding energies of possible  $N^*-^3\text{He}$  states are listed in Table I. As compared to the  $\pi N N^*$  and  $\eta N N^*$  couplings, the  $\pi N^* N^*$  and  $\eta N^* N^*$  couplings are even much less known. In view of the above uncertainties and also the fact that the present work is aimed at finding out how much the  $N^*$  momentum distribution in a nucleus differs from that of a nucleon, we do not attempt a more sophisticated calculation.

### A. Elementary $N N^*$ interaction

The elementary interaction is considered to proceed by the exchange of a pion and an eta meson as shown in Fig. 1. We consider an  $N^*$  which is neutral. The calculation for a positively charged  $N^*$  can be repeated in a similar way. Diagrams involving the  $N^* N^* \pi$  or  $N^* N^* \eta$  couplings which are hardly known will not be considered. Apart from this fact,

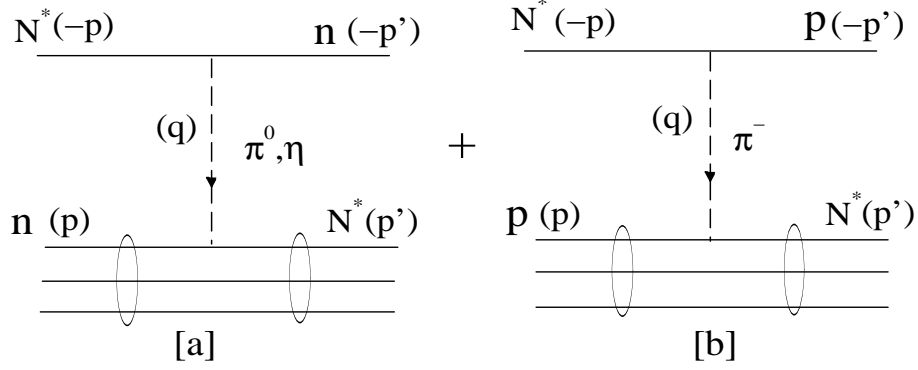


FIG. 1: Elementary  $N N^* \rightarrow N N^*$  processes considered in the interaction of the  $N^*$  with a nucleus.

for such diagrams, the potential turns out to be spin dependent (and so also suppressed as compared to the leading term in the potential of Fig. 1 ).

The  $\pi NN^*$  and  $\eta NN^*$  couplings (with  $N^*(1535, 1/2^-)$ ) are given by the following interaction Hamiltonians [20]:

$$\delta H_{\pi NN^*} = g_{\pi NN^*} \bar{\Psi}_{N^*} \vec{\tau} \Psi_N \cdot \vec{\Phi}_\pi + \text{h.c.} \quad (1)$$

$$\delta H_{\eta NN^*} = g_{\eta NN^*} \bar{\Psi}_{N^*} \Psi_N \cdot \Phi_\eta + \text{h.c.}$$

Let us consider the diagram for the  $N^* n \rightarrow n N^*$  process in Fig. 1 and use the standard Feynman diagram rules with the non-relativistic approximation for the spinors

$$u_i = \sqrt{2m_i} \begin{pmatrix} w_i \\ \frac{\vec{\sigma}_i \cdot \vec{p}_i}{2m_i c} w_i \end{pmatrix}, \quad (2)$$

to write the amplitude as

$$\frac{g_{x NN^*}^2 \bar{u}_{N^*}(\vec{p}') u_n(\vec{p}) \bar{u}_n(-\vec{p}') u_{N^*}(-\vec{p})}{q^2 - m_x^2}, \quad (3)$$

where  $x = \pi$  or  $\eta$  and  $q^2 = \omega^2 - \vec{q}^2$  is the four momentum squared carried by the exchanged meson ( $q = p' - p$  as shown in the figure). Here for example,

$$\bar{u}_n(-\vec{p}') u_{N^*}(-\vec{p}) = N \left( 1 - \frac{\vec{\sigma}_n \cdot \vec{p}' \vec{\sigma}_{N^*} \cdot \vec{p}}{4m_N m_{N^*}^2 c^2} \right) \quad (4)$$

and we drop the second term in the brackets which is spin dependent as well as  $1/c^2$  suppressed. The potential in momentum space obtained from the above amplitude is given as:

$$v_x(q) = \frac{g_{x NN^*}^2}{q^2 - m_x^2} \left( \frac{\Lambda_x^2 - m_x^2}{\Lambda_x^2 - q^2} \right)^2, \quad (5)$$

where the last term in brackets has been introduced to take into account the off-shellness of the exchanged meson. The four momentum transfer squared,  $q^2 = \omega^2 - \vec{q}^2$ , in the present calculation is approximated simply as  $q^2 \simeq -\vec{q}^2$ . Since the mass of the  $N^*$  is much bigger than that of the nucleon, the neglect of the energy transfer,  $\omega$ , in the elastic  $N N^* \rightarrow N N^*$  process as such is not well justified. However we do not expect the relative momentum distribution of the  $N^*$  in the nucleus to depend strongly on the mass of the  $N^*$  (an expectation which will be verified later numerically). We thus proceed further without a non-zero  $\omega$  which would give rise to poles in (5) and make the calculation of the  $N^*$  nucleus potential a formidable task. The potential in (5) is Fourier transformed to obtain the potential in  $r$ -space. The Fourier transform of (5) can be calculated analytically and we get,

$$v_x(r) = \frac{g_{xNN^*}^2}{4\pi} \left[ \frac{1}{r} \left( e^{-\Lambda_x r} - e^{-m_x r} \right) + \frac{\Lambda_x^2 - m_x^2}{2\Lambda_x} e^{-\Lambda_x r} \right]. \quad (6)$$

In order to evaluate the above potential, we need to know the coupling constants at the  $\pi NN^*$  and  $\eta NN^*$  vertices. One can find a range of values in literature as discussed above. In Fig. 2, we see the sensitivity of these potentials to the use of different sets of parameters. Whereas the first two sets are shown to display the sensitivity to the values of the cut-off parameters, the next set is the one which gives the highest binding of the  $N^*$  and nuclei in this work. It gives rise to one bound  $N^*$ - $^3\text{He}$  state at -4.78 MeV and 3 bound  $N^*$ - $^{24}\text{Mg}$  states at -50.3, -22.5 and -3.25 MeV. Using this as well as other sets listed in Table I, we perform an exploratory study of the momentum distributions of the  $N^*$ .

## B. $N^*$ -nucleus potentials

Once the elementary potential has been defined, the folding model with

$$V(R) = \int d^3r \rho(r) v(|\vec{r} - \vec{R}|), \quad (7)$$

is used to construct the  $N^*$  nucleus potential  $V(R)$  which is given by

$$\begin{aligned} V(R) &= V_p(R) + V_n(R) \\ &= Z \int d^3r \rho_p(r) v_p(|\vec{r} - \vec{R}|) + N \int d^3r \rho_n(r) v_n(|\vec{r} - \vec{R}|), \end{aligned} \quad (8)$$

where,  $Z$  and  $N$  are the number of protons and neutrons,  $v_n(r) = v_{\pi^0}(r) + v_\eta(r)$  and due to the isospin factor appearing in the  $\pi^-$  exchange diagram (see Fig. 1 and Eq.(1)),

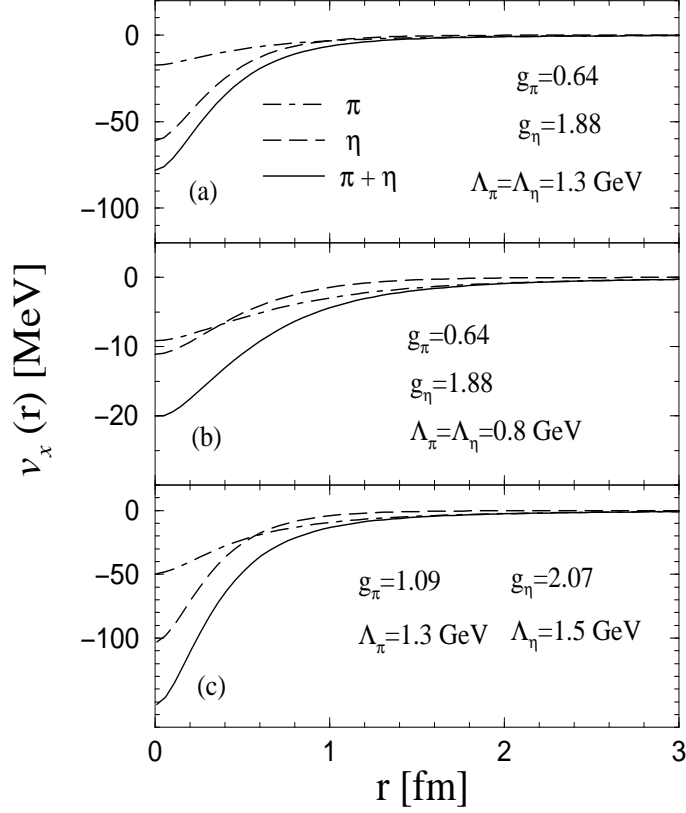


FIG. 2: Elementary potential as given in Eq.(6). Note that whereas  $\pi + \eta$  exchange contributes to the  $n N^* \rightarrow n N^*$  potential, only  $\pi$  contributes to the  $p N^* \rightarrow p N^*$  potential in  $N^* - {}^3\text{He}$ .

$v_p(r) = v_{\pi-}(r) \vec{\tau}_1 \cdot \vec{\tau}_2$ . Note that in the case of  ${}^3\text{He}$  with  $Z = 2$  and due to the isospin factor in  $v_p(r)$ , the contribution of  $V_p(R)$  to the total  $V(R)$  is much larger than that of  $V_n(R)$ . Since  $v_p(r)$  (and hence  $V_p(R)$ ) involves only the pion exchange diagram (Fig. 1[b]), the dominant contribution to the  $N^*$ -nucleus potential comes from pion exchange. Since the pion exchange potential is fairly long range, the folding model chosen in the present work, though not ideal, seems acceptable.

After performing the angle integration, the above integral reduces for example to

$$V_n(R) = \frac{-2\pi A}{R} \int \left\{ \frac{e^{-m_x(|r-R|)} - e^{-m_x(r+R)}}{m_x} - \frac{e^{-\Lambda_x(|r-R|)} - e^{-\Lambda_x(r+R)}}{\Lambda_x} \right. \\ \left. + B \left[ \left( \frac{r+R}{\Lambda_x} + \frac{1}{\Lambda_x^2} \right) e^{-\Lambda_x(r+R)} - \left( \frac{|r-R|}{\Lambda_x} + \frac{1}{\Lambda_x^2} \right) e^{-\Lambda_x|r-R|} \right] \right\} r dr \rho_n(r), \quad (9)$$

where  $A = g_{xNN^*}^2/4\pi$  and  $B = (\Lambda_x^2 - m_x^2)/2\Lambda_x$ .

In case of the  ${}^3\text{He}$  nucleus, the majority of information available in literature is on the charge density distribution of  ${}^3\text{He}$  obtained from electron scattering. The root mean square

radius,  $r_{ch}^{3He} = 1.88 \pm 0.05$  fm, obtained in [8] from the  $^3\text{He}$  charge form factor is a bit smaller than the value of  $1.959 \pm 0.03$  fm in [21]. Ref. [21] also provides the charge form factor of  $^3\text{H}$  with  $r_{ch}^{3H} = 1.755 \pm 0.086$  fm. There exists a parametrization of the matter density given in [22] where a folding model analysis of  $^3\text{He}$  elastic scattering on heavy nuclei is performed. The authors fit the parameters in a gaussian density to reproduce a  $^3\text{He}$  matter radius of 1.68 fm (calculated as  $r_{mat}^2 = r_{ch}^{3He} - r_p^2$  with  $r_p$  being the radius of the proton). There is however no direct experimental data for the neutron density distribution in  $^3\text{He}$ . We identify the neutron density distribution in  $^3\text{He}$  with the proton density in  $^3\text{H}$ , which not only seems reasonable provided that the charge symmetry breaking is small but also agrees with the matter distribution given in [22]. Such an approach of calculating the nuclear densities using the charge densities of  $^3\text{He}$  and  $^3\text{H}$  has also been used earlier in literature [23]. Thus, for the proton density distribution  $\rho_p(r)$ , we choose a sum of Gaussians [21], namely,

$$\rho(r) = \frac{1}{2\pi^{3/2}\gamma^3} \sum_{i=1}^N \frac{Q_i}{1 + 2R_i^2/\gamma^2} \left( e^{-(r-R_i)^2/\gamma^2} + e^{-(r+R_i)^2/\gamma^2} \right), \quad (10)$$

where the parameters  $Q_i$ ,  $R_i$  and  $\gamma$  for  $^3\text{He}$  and  $^3\text{H}$  can be found in [21]. Thus, with  $\rho_p = \rho_{ch}^{3He}$  and  $\rho_n = \rho_{ch}^{3H}$  (both normalized to 1), the above integral can in principle be done analytically. However, the analytic results are lengthy expressions which include error functions and exponentials. They are not particularly enlightening and hence we rather perform the integral numerically. The density for  $^{24}\text{Mg}$  is assumed to have the following Woods-Saxon form [24]:

$$\rho(r) = \frac{\rho_0}{1 + \exp\left(\frac{r-c}{a}\right)}, \quad (11)$$

where  $c = r_A [1 - (\pi^2 a^2 / 3 r_A^2)]$  with  $a = 0.54$  fm and  $r_A = 1.13 A^{1/3}$ . The  $N^*$  nuclear potentials thus evaluated (see [10]) can be fitted reasonably well to Woods Saxon forms of potentials. This fact facilitates the search for a possible  $N^*$ -nucleus bound state and the calculation of its wave function and hence momentum distribution. The potentials corresponding to the various sets of parameters in Table I can be fitted by a Woods Saxon potential with the depth parameter  $V_0$  ranging between 14 to 42 MeV,  $a = 0.8$  fm and  $R$  from 1.15 to 1.34 fm.



TABLE I: The  $\pi NN^*$  and  $\eta NN^*$  coupling constants and the binding energies of the possible  $N^*-^3\text{He}$  bound states obtained with the corresponding set in the  $N N^* \rightarrow N N^*$  potentials.

	$g_{\pi NN^*}$	$g_{\eta NN^*}$	E (MeV)
Chiral constituent quark model fits partial decay widths [16]	1.09	2.07	-4.78
Hidden gauge formalism <sup>†</sup> fits partial widths and $\pi^- p \rightarrow \eta n$ [18]	1.05	1.6	-3.6
vector- and pseudoscalar-baryon coupled channel study [17] <sup>†</sup> $N^*(1535)$ is dynamically generated	0.95	1.77	-2.1
One boson exchange model fits $pp \rightarrow pp\eta$ data [15]	0.8	2.22	-0.8
Data on $\eta$ photoproduction on heavy nuclei [14] fits $p(\gamma, \eta)p$ and $d(\gamma, \eta)np$ data within ELA [19]	0.669	2.005	-0.04

### III. MOMENTUM DISTRIBUTION OF THE $N^*$ IN NUCLEI

The Schrödinger equation for the Woods Saxon potential can be reduced to one for the hypergeometric functions [25] and a condition for the existence of bound states can be found. For a Woods Saxon potential of the type

$$V(r) = -\frac{V_0}{1 + e^{\frac{r-R}{a}}} \quad (12)$$

the Schrödinger equation

$$\frac{d^2 u}{dr^2} + \frac{2}{r} \frac{du}{dr} + \frac{2m}{\hbar^2} (E - V) u = 0 \quad (13)$$

may be transformed to the independent variable  $y = 1/[1 + e^{r-R/a}]$  to obtain a hypergeometric differential equation. After some algebra [25] one obtains the following condition for bound states:

$$\frac{\lambda R}{a} + \Psi - 2\phi - \arctan \frac{\lambda}{\beta} = (2n - 1) \frac{\pi}{2} \quad n = 0, \pm 1, \pm 2, \dots \quad (14)$$

where,

$$\frac{2mE}{\hbar^2} a^2 = -\beta^2; \quad \frac{2mV_0}{\hbar^2} a^2 = \gamma^2; \quad \lambda = \sqrt{\gamma^2 - \beta^2}$$

and  $\phi = \arg\Gamma(\beta + i\lambda)$ ;  $\Psi = \arg\Gamma(2i\lambda)$ .

Defining  $u(r) = \chi(r)/r$  and  $y = 1/[1 + e^{r-R/a}]$ , the solution of the hypergeometric differential equation can be found to be

$$\chi = y^\nu (1 - y)^\mu {}_2F_1(\mu + \nu, \mu + \nu + 1, 2\nu + 1; y) \quad (15)$$

where  $\nu = \beta$  and  $\mu^2 = \beta^2 - \gamma^2$ . Since the variable  $y$  is given in terms of  $r$ , we essentially have the wave function  $\chi(r)$  which can then be Fourier transformed as follows:

$$\chi(p) = \left(\frac{2}{\pi}\right)^{1/2} \int_0^\infty r j_0(pr) \chi(r) dr \quad (16)$$

to evaluate the momentum distribution  $T(p)$  as,

$$T(p) = \frac{1}{4\pi} |\chi(p)|^2 p^2. \quad (17)$$

$T(p)$  is normalized such, that,

$$4\pi \int T(p) dp = 1 \quad (18)$$

Figure 3 displays the relative momentum distribution  $T(p)$  of  $N^*$ - $^3\text{He}$  inside a  $^4\text{He}$  nucleus

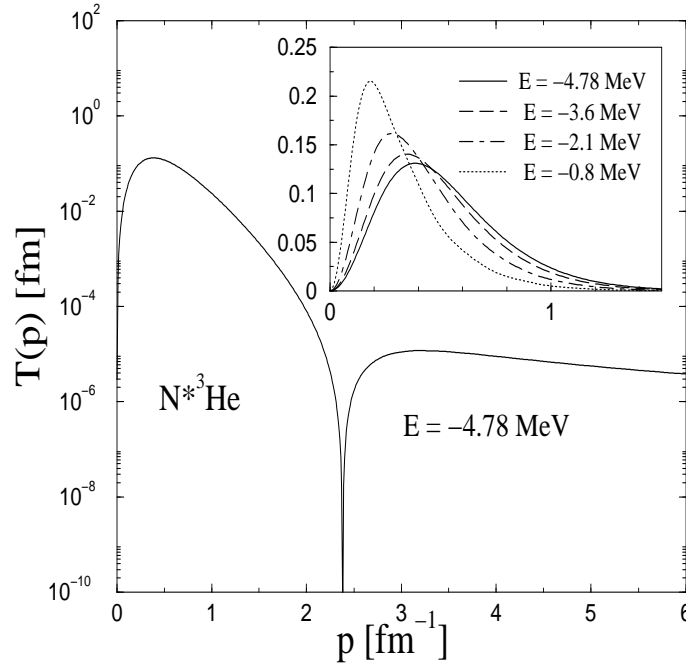


FIG. 3: Momentum distribution of the  $N^*$  in  $^4\text{He}$ . Calculations with different sets of coupling constants (given in Table I) are shown in the inset on a linear scale.

which contains an  $N^*$  instead of a neutron. The curve shown on the logarithmic scale corresponds to the set of parameters in Table I which give the highest binding. The results for other parameter sets in Table I are shown on a linear scale in the inset since one does not see much difference at small momenta on the log scale. The offshell cut-off parameters appearing in the elementary  $N N^* \rightarrow N N^*$  potential are chosen to be  $\Lambda_\pi = 1.3$  GeV and  $\Lambda_\eta = 1.5$  GeV in all cases. Changing the cut-offs to  $\Lambda_\pi = 0.9$  GeV and  $\Lambda_\eta = 1.3$  GeV for example, does not change the distribution significantly (except for a small shift at high momenta) and is hence not shown in the figure.

### A. Dependence on the $N^*$ mass

The  $N^*-^3\text{He}$  potentials do not depend on the mass of the  $N^*$  but in the search for bound states using the condition (14), one has to introduce the  $N^*$  mass to calculate the reduced mass in that expression. In order to check the sensitivity of the results to the choice of the  $N^*$  mass, we varied it between 1400 and 1550 MeV. The corresponding binding energies of states fulfilling the condition (14) varied from 4.34 to 4.84 MeV for the parameter set chosen [16]. This variation introduces a very small change in the form of the bound state wave function as well as momentum distribution as can be seen in Fig. 4[a]. This finding complements earlier results from [14] which indicate little modification of the in-medium excitation of the S11(1535). Though some evidence of broadening was reported in [26], the  $N^*$  mass of 1544 MeV calculated in the Quark Meson Coupling (QMC) model (with the  $N^*$  interpreted as a 3-quark state) [27] seems to be consistent with the former experimental findings as well as the results of the present work.

### B. Comparison with a nucleon momentum distribution in $^4\text{He}$

In order to compare the  $N^*-^3\text{He}$  relative momentum distribution in  $^4\text{He}$  with that of a nucleon in standard  $^4\text{He}$ , we replace the Woods Saxon parameters by  $V_0 = 66$  MeV,  $R = 1.97$  fm and  $a = 0.65$  fm, to get a neutron- $^3\text{He}$  potential which produces a state at -20.6 MeV while fulfilling the condition in (14) with the reduced mass of a neutron and  $^3\text{He}$ . This is indeed close to the energy required to separate a neutron from  $^4\text{He}$ . Even if the curve for the momentum distribution of the neutron calculated in this manner does not

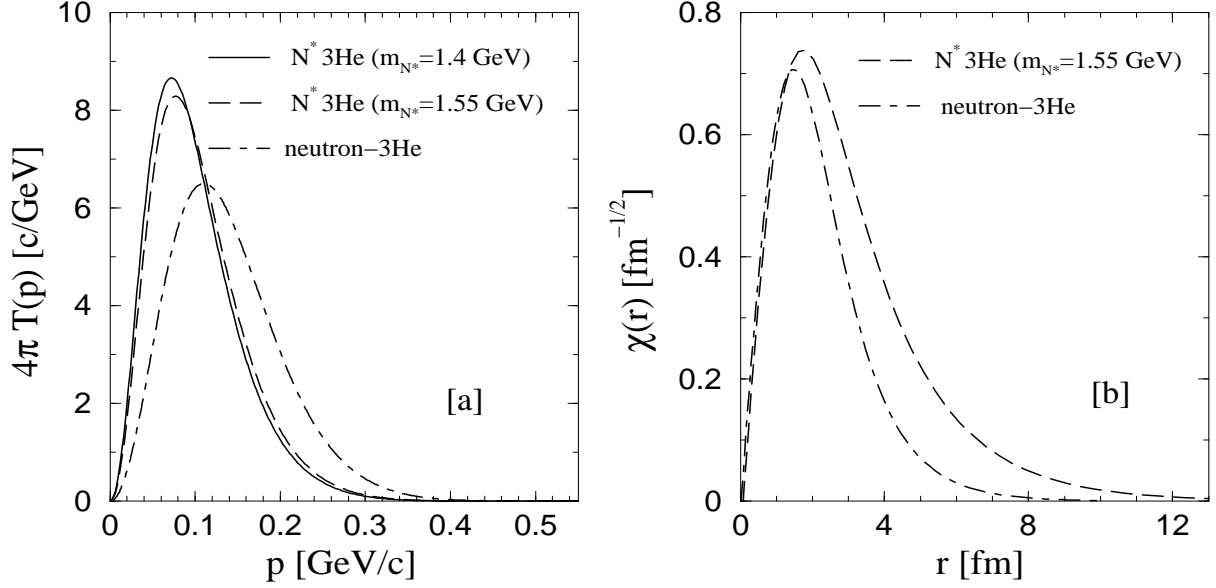


FIG. 4: Variation of the  $N^*$ - $^3\text{He}$  momentum distribution in  $^4\text{He}$  with  $N^*$  mass (solid and dashed lines correspond to 1400 and 1550 MeV respectively in [a]). The dot-dashed line corresponds to [a] the momentum distribution and [b] the wave function of the neutron- $^3\text{He}$  bound state (calculated within the same model). The wave function of  $N^*$ - $^3\text{He}$  (dashed line) for  $m_{N^*} = 1550 \text{ MeV}$  is also shown in [b].

have the authenticity of one evaluated using few body equations, it is pretty close to a realistic calculation [28] (see Fig. 5 and the discussion below) and serves for the purpose of comparison. In Fig. 4[b] we see the difference between the bound wave functions for the  $N^*$ - $^3\text{He}$  and neutron- $^3\text{He}$  systems which explains the difference in the distributions in Fig. 4[a]. With the  $N^*$ - $^3\text{He}$  being loosely bound ( $-4.78 \text{ MeV}$ ) (as compared to the neutron which is bound by  $-20.6 \text{ MeV}$ ), the wave function of the  $N^*$ - $^3\text{He}$  is more spread out in  $r$ -space (Fig. 4[b]). This causes the momentum distribution to be narrower. Other sets of parameters for the  $N N^*$  interaction leading to lesser binding lead to even narrower distributions as seen in the inset in Fig. 3. A better agreement on the  $\pi N N^*$  and  $\eta N N^*$  coupling constants would be useful in order to perform a more accurate estimate of the momentum distribution of the  $N^*$  in the nucleus.

In order to test the validity of the calculations done in the present work, we repeat a similar calculation for the proton- $^3\text{H}$  system in  $^4\text{He}$  for which some results using few body equations exist in literature. Though the momentum distribution for  $n$ - $^3\text{He}$  is not

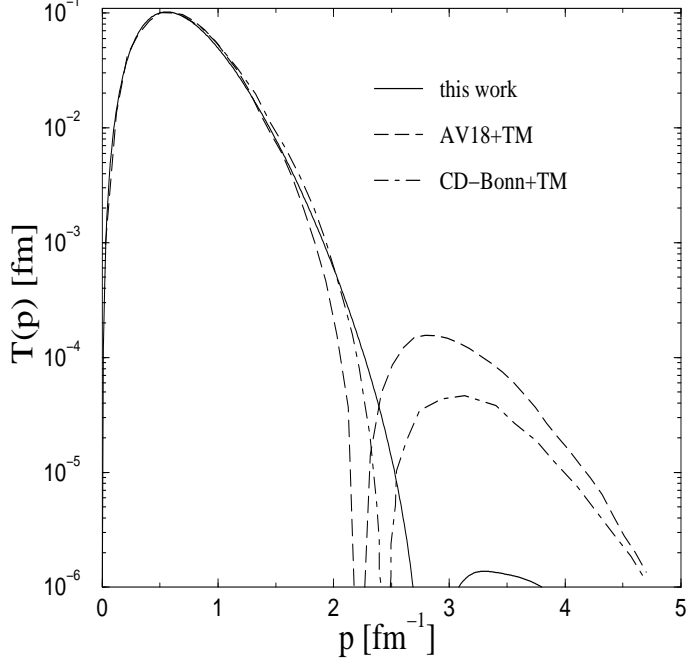


FIG. 5: Comparison of the proton- $^3\text{H}$  momentum distribution in  $^4\text{He}$  of the present work (solid line) with others calculated using Faddeev-Yakubovsky equations [28] with the AV18+TM (dashed) and CD-Bonn+TM (dot-dashed) potentials.

expected to be very different from that of  $p$ - $^3\text{H}$  in  $^4\text{He}$ , we perform this calculation in order to compare with the available few-body results. With the Woods Saxon parameters of  $V_0 = 66$  MeV,  $R = 1.93$  fm and  $a = 0.65$  fm which reproduce the  $p$ - $^3\text{H}$  binding of 19.8 MeV, we obtain a distribution which agrees at small and medium momenta with more sophisticated calculations [28] shown in Fig. 5. The disagreement is only in the region of large momenta where the magnitude of  $T(p)$  has fallen down by three orders of magnitude. Thus, the conclusion that the  $\text{N}^*$ - $^3\text{He}$  momentum distribution is narrower than the neutron- $^3\text{He}$  distribution, drawn from the calculations of the present work seems quite reliable.

### C. $\text{N}^*$ - $^{24}\text{Mg}$ bound states

Using the set of parameters from [16] for the  $\pi\text{NN}^*$  and  $\eta\text{NN}^*$  coupling constants, the condition (14) allows three bound states of  $\text{N}^*$ - $^{24}\text{Mg}$  at energies of -50.3, -22.5 and -3.25 MeV for  $n = 1, 2$  and 3 respectively. The Woods Saxon potential parameters of the  $\text{N}^*$ -

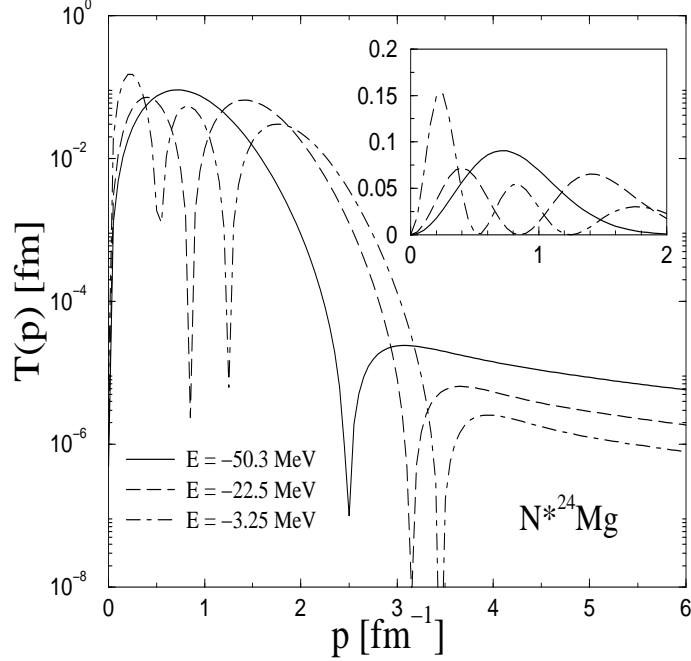


FIG. 6:  $N^*-^{24}\text{Mg}$  momentum distribution in  $^{25}\text{Mg}$  for three possible binding energies corresponding to the number of nodes  $n = 1, 2$  and  $3$  in the bound wave functions.

$^{24}\text{Mg}$  system are:  $V_0 = 80$  MeV,  $a = 0.97$  fm and  $R = 2.85$  fm. In Fig. 6 one can see the distributions with one, two and three nodes accordingly.

#### IV. SUMMARY

The broad S11 baryon resonance  $N^*(1535)$  enters as one of the most essential ingredient in reactions involving the production of the neutral pseudoscalar eta meson ( $\eta$ ) and hence also in the analyses of possible eta-mesic nuclei. Since the low energy  $\eta N$  interaction predominantly proceeds by producing an  $N^*$  resonance which propagates, decays and regenerates inside the nucleus, it seems legitimate to ponder about the possible existence of an  $N^*$ -nucleus bound state too. Indeed, performing such an investigation in [10], it was found that depending on the strength of the  $N N^*$  interaction, loosely bound, broad quasibound states of the  $N^*$  with  $^3\text{He}$  and  $^{24}\text{Mg}$  nuclei can be formed. In the present work, the investigation is continued to evaluate the momentum distribution of such an  $N^*$  inside the nucleus. Being aware of the fact that neither does any experimental evidence of  $N^*$ -nuclei exist nor is the  $N N^*$  interaction accurately known, the calculations are done within a folding model

where the elementary  $N N^* \rightarrow N N^*$  potential is folded with the known nuclear densities. The present work finds that since the  $N^*$  is loosely (or even very loosely, depending on the  $\pi NN^*$  and  $\eta NN^*$  couplings) bound to a nucleus, the bound state wave function of an  $N^*$  as compared to that of a nucleon is more spread out in  $r$ -space and hence the momentum distribution is narrower than in case of the nucleon. This finding is important in view of the fact that experimental analyses generally approximate the momentum distribution of an  $N^*$  by that of a nucleon in a nucleus. The present work is a first attempt to evaluate the  $N^*(1535)$  resonance momentum distribution in nuclei. This distribution, as mentioned in the beginning, is necessary to establish the detector system acceptance for the registration of the  $dd \rightarrow (^3\text{He}-N^*) \rightarrow ^3\text{He } N\pi$  reaction and to determine the data selection criteria [6]. A calculation of the momentum distribution of  $N^*$ -d in  $^3\text{He}$  would be necessary for the analysis of the  $pd \rightarrow (d-N^*) \rightarrow d N\pi$  reaction aimed at searching  $\eta$ -mesic  $^3\text{He}$  whose prospects seem higher due to the fact that we have already seen a strong enhancement in the  $pd \rightarrow ^3\text{He } \eta$  reaction near threshold. Such a calculation would however be better performed using a few body formalism for the  $N^*$ -p-n system. An improved knowledge of the  $N^*$  coupling constants and experimental searches of  $N^*$  nuclei could motivate such sophisticated few body calculations in future.

### Acknowledgments

The author thanks Prof. Pawel Moskal for useful comments and discussions. The author also thanks the Faculty of Science at the University of Los Andes, Colombia for financial support (project no. P15.160322.009/01-01-FISI02).

- 
- [1] R. S. Bhalerao and L. C. Liu, *Phys. Rev. Lett.* **54**, 865 (1985).
  - [2] H. Machner, *J.Phys. G* **42** 043001 (2015); B. Krusche, C. Wilkin, *Prog. Part. Nucl. Phys.* **80**, 43 (2014); Q. Haider and L. C. Liu, *Int. J.Mod. Phys E* **24**, 1530009 (2015).
  - [3] N. G. Kelkar, K. P. Khemchandani, N. J. Upadhyay and B. K. Jain, *Rep. Prog. Phys.* **76**, 066301 (2013).
  - [4] M. Pfeiffer *et al.*, *Phys. Rev. Lett.* **92**, 252001 (2004); G. A. Sokol and L. N. Pavlyuchenko, *Phys. Atom. Nucl* **71**, 509 (2008).

- [5] S. D. Bass, *Hyperfine Int.* **234**, 41 (2015); S.D. Bass and P. Moskal, *Acta Phys. Pol. B* **47**, 373 (2016); H. Fujioka *et al.* (for Super-FRS collaboration), *Hyperfine Int.* **234**, 33 (2015).
- [6] W. Krzemien, P. Moskal and M. Skurzok, *Acta Phys. Polon. B* **46** 757 (2015); M. Skurzok, W. Krzemien, O. Rundel and P. Moskal, *EPJ Web Conf.* **117**, 02005 (2016); P. Adlarson *et al.*, *Phys. Rev. C* **87**, 035204 (2013).
- [7] S. Wycech, A. M. Green and J. A. Niskanen, *Phys. Rev. C* **52**, 544 (1995); S. Wycech and A. M. Green, *Int. J. Mod. Phys. A* **20**, 637 (2005); N. G. Kelkar, K. P. Khemchandani and B. K. Jain, *J. Phys. G* **32**, 1157 (2006); N. G. Kelkar, *Phys. Rev. Lett.* **99**, 210403 (2007).
- [8] J. S. McCarthy, I. Sick and R. R. Whitney, *Phys. Rev. C* **15**, 1396 (1977).
- [9] M. Skurzok, Ph.D. thesis, Jagiellonian University (2015), arXiv:1509.01385.
- [10] N. G. Kelkar, D. Bedoya Fierro and P. Moskal, *Acta Phys. Pol. B* **47**, 299 (2016).
- [11] P. Bartsch *et al.*, *Eur. Phys. J. A* **4**, 209 (1999); T. Walcher, *Phys. Rev. C* **63**, 064605 (2001); C. Chumillas, A. Parreño and A. Ramos, *Nucl. Phys. A* **791**, 329 (2007).
- [12] M. Dillig, *Phys. Rev. C* **14**, 2226 (1976).
- [13] A. B. Santra and B. K. Jain, *Nucl. Phys. A* **634**, 309 (1998); W. Peters, U. Mosel and A. Engel, *Z. Phys. A* **353**, 333 (1996); Ju-Jun Xie, Bing-Song Zou and Huon-Ching Chiang, *Phys. Rev. C* **77**, 015206 (2008); A. Fix and H. Arenhövel, *Nucl. Phys. A* **697**, 277 (2002).
- [14] M. Röbig-Landau *et al.*, *Phys. Lett. B* **373**, 45 (1996); R. Auerbeck *et al.*, *Z. Phys. A* **359**, 65 (1997).
- [15] T. Vetter, A. Engel, T. Biró and U. Mosel, *Phys. Lett. B* **263**, 153 (1991); A. Moalem, E. Gedalin, L. Razdolskaja and Z. Shorer, *Nucl. Phys. A* **589**, 649 (1995).
- [16] C. S. An and B. Saghai, *Phys. Rev. C* **84**, 045204 (2011).
- [17] K. P. Khemchandani, A. Martínez Torres, H. Nagahiro and A. Hosaka, *Phys. Rev. D* **88**, 114016 (2013).
- [18] E. J. Garzon and E. Oset, *Phys. Rev. C* **91**, 025201 (2015).
- [19] R. C. Carrasco, *Phys. Rev. C* **48**, 2333 (1993).
- [20] B. Lopez Alvaredo and E. Oset, *Phys. Lett. B* **324**, 125 (1994).
- [21] A. Amroun *et al.*, *Nucl. Phys. A* **579**, 596 (1994).
- [22] J. Cook and R. J. Griffiths, *Nucl. Phys. A* **366**, 27 (1981).
- [23] D. H. Lu, K. Tsushima, A. W. Thomas, A. G. Williams and K. Saito, *Phys. Lett. B* **441**, 27 (1998).



- [24] P. Roy Chowdhury, C. Samanta and D. N. Basu, Phys. Rev. C **73**, 014612 (2006); D. K. Srivastava, D. N. Basu and N. K. Ganguly, Phys. Lett. B **124**, 6 (1983).
- [25] S. Flügge, *Practical Quantum Mechanics*, Springer (1998); M. Ghominejad, Eur. Phys. J. Plus **128**, 59 (2013).
- [26] T. Yorita *et al.*, Phys. Lett. B **476**, 226 (2000).
- [27] Steven D. Bass and Anthony W. Thomas, Phys. Lett. B **634**, 368 (2006).
- [28] A. Nogga, H. Kamada, W. Glöckle and B. R. Barrett, Phys. Rev. C **65**, 054003 (2002); A. Nogga, “Nuclear and hypernuclear 3 and 4 body bound states”, Ph. D. thesis, Ruhr Universität, Bochum, 2001 (available at <http://www-brs.ub.ruhr-uni-bochum.de/netahtml/HSS/Diss/NoggaAndreas/>).